

See discussions, stats, and author profiles for this publication at: <https://www.researchgate.net/publication/8537020>

Recognition of Anionic Phospholipid Membranes by an Antihemostatic Protein from a Blood-Feeding Insect

ARTICLE *in* BIOCHEMISTRY · JULY 2004

Impact Factor: 3.02 · DOI: 10.1021/bi049655t · Source: PubMed

CITATIONS

60

READS

16

5 AUTHORS, INCLUDING:



John F Andersen

National Institutes of Health

110 PUBLICATIONS 5,409 CITATIONS

SEE PROFILE



Ivo M B Francischetti

National Institutes of Health

126 PUBLICATIONS 5,553 CITATIONS

SEE PROFILE



Jesus G. Valenzuela

National Institute of Allergy and Infectious Di...

182 PUBLICATIONS 7,157 CITATIONS

SEE PROFILE

Published in final edited form as:

Biochemistry. 2004 June 8; 43(22): 6987–6994. doi:10.1021/bi049655t.

Recognition of Anionic Phospholipid Membranes by an Antihemostatic Protein from a Blood-Feeding Insect

John F. Andersen^{*}, Nanda P. Gudderra, Ivo M. B. Francischetti, Jesus G. Valenzuela, and José M. C. Ribeiro

Laboratory of Malaria and Vector Research, National Institutes of Health, NIAID, Bethesda, MD 20892, USA

Abstract

The saliva of blood-feeding insects contains a variety of molecules having antihemostatic activity. Here we describe nitrophorin 7 (NP7), a salivary protein that binds with high affinity to anionic phospholipid membranes. The protein is apparently targeted to the negatively charged surfaces of activated platelets and other cells where it can serve as a vasodilator, antihistamine, platelet aggregation inhibitor, and anticoagulant. As with other members of the nitrophorin group, NP7 reversibly binds a molecule of NO and binds histamine with high affinity. The protein differs from other nitrophorins in that it binds to membranes containing phosphatidylserine. Sedimentation and surface plasmon resonance experiments, revealed two classes of phospholipid binding site having K_d values of 4.8 and 755 nM. NP7 inhibits prothrombin activation by blocking phospholipid binding sites for the prothrombinase complex on the surfaces of vesicles and activated platelets. As a NO complex, NP7 inhibits collagen and ADP-induced platelet aggregation and induces disaggregation of ADP-stimulated platelets by an NO-mediated mechanism. Molecular modeling of NP7 revealed a putative, positively charged membrane interaction surface comprised mainly of a helix lying outside of the lipocalin β -barrel structure.

Keywords

Nitric oxide; histamine; prothrombinase; phosphatidylserine; *Rhodnius prolixus*

Platelet activation is an early event in the response to vascular injury. Resting platelets adhere to the extracellular matrix at a wound site via surface receptors interacting with collagen and von Willebrand factor (1). Signaling through these receptors induces the surface exposure and conformational activation of integrins along with release of thromboxane A2 and secretory granules containing agonists such as ADP, serotonin, and epinephrine (1,2). Protease activated receptor (PAR) pathways activated by circulating thrombin also contribute to these processes (3). Increased adhesion of activated platelets to the extracellular matrix and crosslinking via the interaction of GP IIb-IIIa with circulating fibrinogen leads to the formation of a platelet plug. The plug is both a physical obstruction to blood loss and a substrate for the reactions of the coagulation cascade that lead to fibrin clot formation (1).

Activated platelets undergo changes in the plasma membrane that promote assembly of coagulation complexes at the wound site and allow the formation of a fibrin clot. Normally,

^{*}To whom correspondence should be addressed. John F. Andersen, NIH, NIAID, Laboratory of Malaria and Vector Research, 4 Center Drive, Bldg. 4, Rm. 126, Bethesda, MD 20892. Tel: 301-435-2967. Fax: 301-402-2201. jandersen@niaid.nih.gov.

²The complete cDNA sequence of nitrophorin 7 has been deposited in GenBank with the accession number AY585746.

the membrane bilayer is asymmetric with anionic phospholipids, particularly phosphatidylserine (PS), being sequestered in the inner leaflet through the action of aminophospholipid translocase (4,5). Activation by collagen or thrombin leads to an increase in intracellular calcium concentration and rapid loss of membrane asymmetry through the downregulation of aminophospholipid translocase and the activation of phospholipid scramblase (4,5). The resulting negatively charged exterior surface is essential for the binding and assembly of coagulation factors that make up the factor Xase and prothrombinase complexes. In this way, the exposure of anionic phospholipids in activated platelets serves a regulatory role in hemostasis by labeling the appropriate sites for the initiation of fibrin formation. Other cell types also lose membrane asymmetry when activated. For example, on stimulation with antigen, mast cells rapidly degranulate by a mechanism which results in PS exposure at the site of granule release (6,7).

Blood-feeding arthropods produce many salivary substances that inhibit normal hemostasis, and are necessary for unimpaired blood feeding. Recognition of, and binding to, the anionic surfaces of activated platelets would potentially increase the effectiveness of antihemostatic proteins by targeting them to regions where hemostatic reactions are actively occurring. An important group of antihemostatic proteins in the insect *Rhodnius prolixus* are the nitrophorins (NPs) (8,9). NPs belong to the lipocalin protein family (10,11) and bind a heme moiety in the central cavity of the protein formed by the β -barrel structure (12). The heme is tethered to the protein by a histidine residue that forms the proximal axial iron ligand. NPs are present as NO complexes in the salivary gland, which dissociate to release a single molecule of NO per protein molecule when injected into the host with the saliva (8,13). The NO moves to the vascular endothelium where it traverses cell membranes and activates soluble guanylate cyclase, leading to relaxation of the vascular wall and increased blood flow. NO is also a potent inhibitor of platelet aggregation and acts to reverse the aggregation of platelets stimulated with ADP. Beside the transport of NO, other functions have been ascribed to members of the nitrophorin group. NP2 binds with high affinity to coagulation factor IXa and inhibits the assembly and activity of the intrinsic factor Xase complex (14,15). Also, all NPs are capable of binding a molecule of histamine in the distal pocket after release of NO. It is thought that this process may serve an antiinflammatory function during feeding (16).

In this study, we describe a novel NP that differs from other members of the group by binding with high affinity to PS-containing membranes. The protein contains a positively charged helical region representing a novel PS binding motif. When bound to the membrane, NP7 inhibits clotting by competing for coagulation factor binding sites. NP7 is also shown to be an effective platelet aggregation inhibitor, a function that may be enhanced by recognition and binding with anionic surfaces of activated platelets in the immediate vicinity of a feeding bite.

MATERIALS AND METHODS

Materials

Dimyristoyl L- α -phosphatidylcholine and dipalmitoyl L- α -phosphatidyl-L-serine were purchased from Sigma Chemical Company. S-nitroso-N-acetylpenicillamine (SNAP) was from Molecular Probes Inc. The chromogenic substrate S-2238 (Chromogenix) was from Diapharma. Human coagulation factors Va, Xa, thrombin and prothrombin were obtained from Haematologic Technologies, and collagen was from Chrono-Log Corp.

Cloning and Expression of NP7

The cDNA for nitrophorin 7 (NP7) was obtained as part of a salivary gland EST sequencing project from a library described previously (17). The most likely signal sequence cleavage site of the clone was determined using the SignalP webserver (18). The cDNA was modified to remove the signal sequence, cloned into expression vector pET17b, and expressed in *Escherichia coli* as previously described for nitrophorins 1–4 (9,19). The NP7 protein was obtained as inclusion bodies and was denatured, refolded, and reconstituted with heme as described for other NP. The refolded reconstituted protein was purified by a two-step procedure. First, the protein was dialyzed against 10 mM sodium phosphate pH 6.0 and applied to an SP-Sepharose column equilibrated in the same buffer. The protein was eluted with a gradient of 0–1M NaCl in 10 mM sodium phosphate pH 6.0. After concentration, the protein was applied to a Sephacryl S-100 column equilibrated with 40 mM Tris-HCl, pH 7.4, 150 mM NaCl (TBS) and eluted with the same buffer. The purity and quality of the preparations were determined by SDS-PAGE and spectral measurements. Recombinant NP1, NP2, and NP3 were prepared as described previously (9,19).

A site-directed mutant (K149A) of NP7 was constructed using a two-step PCR procedure, and was expressed, refolded, reconstituted with heme, and purified using the same methods as for wild-type NP7.

Vesicle Formation and Protein Binding

Large unilamellar vesicles were formed by injection of chloroform solutions of phospholipids into 20 mM Tris-HCl, pH 7.5 at 70°C (20). The final concentration of the vesicle suspensions was 1 mg/ml, and nitrogen was bubbled through the mixture during preparation. Binding was measured at various salt concentrations by diluting the vesicle suspension 2-fold in TBS containing the appropriate concentration of NaCl and 2 μ NP7 in a final volume of 50 μ l. The mixtures were incubated at room temperature for 30 min and centrifuged at 100,000 $\times g$ for 30 min. The supernatant was removed and the pellet was resuspended in 50 μ l of TBS. Both the pellet and supernatant fractions were analyzed by SDS-PAGE and the fraction of bound protein was determined by densitometry of Coomassie blue-stained gels using the program ImageJ (available at <http://rsb.info.nih.gov/ij/>).

Surface Plasmon Resonance

A phosphatidylcholine (PC):PS (3:1) monolayer was formed on a BIAcore HPA hydrophobic sensor chip by passing a 1 mg/ml suspension of vesicles in 40 mM Hepes, pH 7.4, 150 mM NaCl (HBS) over the chip surface at 10 μ l/min for 30 min. This was followed by two 20 s washes with 10 mM NaOH flowing at 20 μ l/min. Surface plasmon resonance (SPR) responses of NP7 binding to the prepared monolayer were measured using a BIAcore 2000 instrument at a flow rate of 30 μ l/min using HBS buffer. Between runs, the monolayer was regenerated by injecting 10 mM NaOH at a flow rate of 30 μ l/min for 10 s. Rate constants for binding and release were obtained by fitting the data with a two-binding site, parallel reaction model contained in the BIAcore evaluation package.

Recalcification Time of Platelet-rich Plasma

Platelet rich plasma (PRP) was obtained by platelet-pheresis at the NIH blood bank. To measure recalcification time, 50 μ l of PRP was diluted with 150 μ l of calcium-free Tyrode buffer. NP7 was added to the desired concentration and the mixture was incubated for 1 min at 37 °C. At this point, 50 μ l 25 mM CaCl₂ in Tyrode buffer was added and the tubes were incubated at 37 °C until visible clots appeared.

Inhibition of Prothrombinase Reaction

The inhibition by NP7 of prothrombin activation by reconstituted prothrombinase complex was evaluated in the presence of different phospholipid compositions and concentrations. All reactions were performed in 40 mM Tris-HCl, pH 7.4, 150 mM NaCl, 0.5 mM CaCl₂ in 96-well microtiter plates. Each well contained buffer, 250 pM factor Xa, 1 nM factor Va, and phospholipid vesicles prepared as described above in a final volume of 130 μ l. To start the reaction, prothrombin was added to a concentration of 1.2 μ M followed by incubation of the plate for 20 min at 37 °C. To stop the reaction, 50 μ l of each mixture was added to 150 μ l of 40 mM Tris-HCl, pH 7.4, 150 mM NaCl, 5 mM EDTA. The thrombin concentration was measured by following hydrolysis of the chromogenic substrate S-2238 (180 μ M) in a microtiter plate reader (405 nm) at 25 °C. When activated washed platelets (see below for preparation) were used as a source of phospholipid, 5 μ g of collagen was added to 1 ml of washed platelets. To each prothrombinase reaction, 5 μ l of platelet suspension (approximately 1.5×10^6 platelets) was added.

Inhibition of Platelet Aggregation

Washed platelets were prepared from PRP as described previously (21). Aggregation of washed platelets (200,000–400,000/ μ l, suspended in Tyrode buffer without calcium and containing 1 mg/ml BSA) was measured 37 °C in a Chrono-Log aggregometer using either ADP or collagen to initiate aggregation. The NP7-NO complex was formed by adding 200 μ M SNAP to a solution of NP7 (50 μ M) in 20 mM sodium acetate, pH 4.5, 150 mM NaCl. The formation of complex was monitored spectrophotometrically. The fully-formed complex was separated from residual SNAP and from free NO by gel filtration on Superdex 75, using the pH 4.5 sodium acetate/NaCl buffer for elution. At this pH, the NP-NO complex is stable as verified spectrophotometrically after chromatography.

Molecular Modeling

The structure of NP7 was modeled based on the crystal structure of NP2 (22) using the Swiss-Model server. After amino acid substitution, the model was energy minimized by 200 cycles of steepest descents, followed by 300 cycles of conjugate gradient minimization. The heme moiety was added to the model manually, using superposition with the crystal structure of NP2 in Insight II. An electrostatic potential grid was calculated using DelPhi (23). Heme was modeled by placing a net charge of +1 on the iron atom (to represent the overall +1 charge of Fe(III) heme) and a charge of $-1/2$ on each of the propionate oxygen atoms. The electrostatic surface was generated using GRASP (24).

RESULTS

Identification and Cloning of NP7

NP7 was identified in a search of expressed sequence tags for peptides with elevated isoelectric points or tracts of basic residues that might be involved in interaction with anionic membranes. The NP7 cDNA encodes a mature polypeptide having a molecular mass of 20.6 kDa if the signal sequence cleavage point predicted by Signal-P is considered to be accurate. The isoelectric point calculated from the NP7 sequence is 8.72, while those of NP1, NP2, NP3, and NP4 are 6.59, 6.34, 6.73, and 6.58, respectively. Of the four major NPs, NP7 is most similar to NP2 and NP3 (Figure 1).

Ligand Binding and Spectral Properties

The physical properties of recombinant NP7 were similar to those of previously described NPs (9,19). The absorbance spectrum of the protein shows a Soret maximum at 403 nm, which is shifted to 420 nm in the NO complex (Figure 2). A histamine complex was also

formed, with the Soret maximum shifted to 412 nm (Figure 2). As previously noted for other NPs, the NO complex was more stable at pH 4–5 than at physiologic pH. In pH 4.5 sodium acetate buffer, a complex formed by incubation with SNAP was stable for several hours at room temperature, was purified by gel filtration chromatography at pH 4.5, and maintained indefinitely at -20°C . Raising the pH of the complex solution by adding concentrated Tris-HCl, pH 7.5 resulted in dissociation of the complex over a period of 10–15 min.

Binding to Phospholipid Vesicles

A sedimentation assay was developed in which lipid-bound and soluble NP7 were quantified by SDS-PAGE and Coomassie blue staining. NP7 was found to bind to phospholipid vesicles containing 100 % PS, but not to those containing only PC (Figure 3a). The binding of NP7 to anionic membranes was dependent on the salt concentration, with complete binding occurring in the absence of sodium chloride and no detectable binding at 640 mM sodium chloride (Figure 3a). In mixed vesicles containing 3:1 PC:PS, the salt concentration required for 50% dissociation was reduced from 385 mM, as seen with 100% PS vesicles, to 175 mM, suggesting a reduction in binding affinity or in the number of available binding sites (Figure 3b). At 150 mM ionic strength, the binding levels were 99% and 64% for PS and PC:PS vesicles, respectively, indicating that NP7 binding occurs under physiologic conditions.

NP1, NP2, and NP3 did not bind to vesicles regardless of salt concentration or phospholipid composition, indicating that interaction with anionic membranes is a specific feature of NP7 that is not seen with other previously characterized forms of NP (Figure 2b).

Binding of NP7 with a 3:1 PC:PS monolayer was detectable by SPR at nanomolar concentrations of ligand at 25°C and 150 mM ionic strength. Biphasic release kinetics were observed at all tested NP concentrations, and kinetic constants were determined by global analysis of the data using a two-binding site, parallel reaction model (Figure 3c; Table 1). The dissociation constants of both modeled binding sites were submicromolar and differed by approximately 150-fold in affinity, suggesting that the binding interaction would be relevant at the low concentrations of salivary protein present in host blood during feeding. NP3, a protein that showed no binding in the sedimentation assay, showed little affinity for the monolayer, further demonstrating the specificity of the interaction of NP7 with anionic membranes.

Inhibition of Recalcification Time

NP7 caused a two-fold delay in the clotting of PRP at $2\text{ }\mu\text{M}$ NP7 and up to five-fold at $10\text{ }\mu\text{M}$ NP7 (Figure 4a). No delay in clotting was seen when NP1 was tested in place of NP7, demonstrating that a protein that does not bind to anionic membranes is also not an inhibitor of coagulation (Figure 4a).

Inhibition of Prothrombinase Activity

NP7 inhibited the activation of prothrombin by reconstituted prothrombinase with an IC_{50} of 42 nM at $0.5\text{ }\mu\text{M}$ PS (Figure 4b). The protein had no effect, however, on the amidolytic activities of thrombin or factor Xa (data not shown). The inhibition of prothrombinase decreased approximately six-fold when the PS concentration was increased three-fold, suggesting that the anticoagulant effect could be overcome by an increase in the number of coagulation complex binding sites (Figure 4b). The phospholipid concentration dependence of inhibition at a single concentration of NP7 (230 nM) showed a clear reduction in inhibition with increasing phospholipid concentration (Figure 4c). This observation demonstrates that competition with the coagulation complex for membrane binding sites is indeed the mechanism of inhibition for NP7.

The prothrombinase complex was also inhibited using mixed vesicles containing a 3:1 ratio of PC to PS. In this case, the IC_{50} for inhibition was elevated to $\sim 1.2 \mu M$ in the presence of $1.5 \mu M$ phospholipids, suggesting the presence of lower affinity binding sites in mixed vesicles (Figure 4d). When washed platelets activated with collagen were used in place of phospholipid vesicles, results were similar to those obtained with mixed vesicles (Figure 4d, $IC_{50} \sim 1.1 \mu M$), indicating that NP7 binds to membranes of physiologically relevant composition as well as to artificial vesicles.

Inhibition of Platelet Aggregation

Although an antiaggregatory function of NPs could be predicted from the NO transport capabilities of these proteins, it has not been explicitly demonstrated in previous studies. Here we found NP7-NO complex to inhibit platelet aggregation at concentrations as low as 10 nM when platelets were stimulated with $3 \mu M$ ADP (Figure 5, traces a–e). The initial shape change response was not inhibited at low concentrations of complex, and only disappeared at higher concentrations (400 nM). If the NP7-NO complex (400 nM) was added to a platelet preparation at the point of maximal ADP-induced aggregation, rapid disaggregation was observed (Figure 5, traces f and g).

At threshold levels of collagen ($0.7 \mu g/ml$), the results were similar to those obtained with ADP; thus, aggregation but not shape change was inhibited at low concentrations of complex. At higher collagen concentrations ($3.3 \mu g/ml$) aggregation could not be reversed, but could be prevented by adding NP7-NO complex at concentrations of 250 nM or greater prior to addition of agonist. When tested at a concentration of 400 nM, the NO-free protein had no effect on either ADP or collagen-induced aggregation, while addition of the same concentration of complex reduced platelet aggregation by 90 % ($N=3$). This verifies that NO was indeed the active agent in inhibiting collagen-induced platelet aggregation.

Molecular Modeling

Comparisons of the electrostatic surface map of the NP7 model with the surfaces of NP1, NP2, and NP4 were made to locate a probable phospholipid interaction region on the NP7 surface. Amino acid alignment of NP sequences showed that a basic region corresponding to an α -helix lying outside of the lipocalin β -barrel is a focus of positive electrostatic potential in NP7 (Figure 1). Indeed, the surface in the vicinity of this helix shows a highly positive electrostatic potential, while the corresponding surface of NP2 does not (Figure 6a). In the NP7 model, five lysine residues are arranged along the helix with their side chains directed toward the solvent (Figure 6b). Interaction with the phospholipid membrane via this surface would direct the opening of the ligand-binding pocket of NP7 away from the membrane, allowing release of NO in the direct vicinity of the membrane surface.

A mutant of NP7 was constructed in which alanine was substituted for lysine at position 149 (Figure 1; numbering does not include signal peptide). In the sedimentation assay described above, using 3:1 PC:PS vesicles, binding was reduced by a factor of three from that observed with wild-type protein, suggesting that this region does play an important role in phospholipid binding (Figure 7).

DISCUSSION

Binding of NP7 to Anionic Membranes and the Delivery of NO to the Host

In platelets and mast cells, the loss of membrane asymmetry is rapid and tightly coupled with other activation events, making it a highly reliable indicator of hemostatic activity and degranulation. Recognition of PS exposure by proteins is important in biologic processes such as the assembly of coagulation complexes and the clearance of apoptotic cells by

macrophages (25,26). The data presented here suggest that the antihemostatic protein NP7 from *R. prolixus* saliva recognizes anionic membranes as an indicator of activation and uses this as a means of targeting the surfaces of activated platelets and degranulating mast cells. Once bound on an activated platelet, the protein can release NO to inhibit platelet aggregation, bind histamine, and act as an anticoagulant by blocking coagulation-factor binding sites.

NP7 carries the potent platelet aggregation inhibitor NO into the host circulation where it is released. NO is highly labile, having a measured lifetime in solution of a few seconds, but is protected from oxidation when bound to NPs (13). Targeted delivery to activated surfaces at the point of feeding may enhance the activity of NP7 as a platelet aggregation inhibitor by delivering NO in a protected form to its site of action and preventing its removal from the feeding area by diffusion and blood flow. Since NO is quite effective in reversing ADP-induced aggregation, NP7 may bind with nascent aggregates at the site of feeding and act to disperse them. After membrane binding and NO release, NP7 is free to bind a molecule of histamine, and may interact directly with exposed PS on degranulating mast cells, thereby increasing the effective concentration of the protein around the point of histamine release. The more abundant NPs 1 to 4 do not bind to membranes, and would therefore remain in solution, diffusing away from the feeding site while releasing NO over a larger area. These proteins may be primarily responsible for causing extensive vasodilation and enhanced blood flow to the feeding site, while the less abundant NP7 remains in the vicinity of the feeding wound and acts primarily as a platelet aggregation inhibitor, antihistamine, and anticoagulant.

Anticoagulant Activity of NP7

Inhibition of coagulation by *R. prolixus* saliva is known to be mediated by the factor Xase complex inhibitor NP2 (14). This protein acts by directly binding with factor IX and IXa, inhibiting the assembly of the complex on the phospholipid membrane; however, it shows no activity against the prothrombinase complex (14). The action of NP7 represents a second mechanism of coagulation inhibition in *R. prolixus*, that of competition with phospholipid-dependent coagulation complexes for membrane binding sites.

Here we show that the activity of the prothrombinase complex is inhibited by NP7 and preliminary results (J.F.A., unpublished results) indicate that the intrinsic factor Xase reaction is inhibited in a manner similar to that of prothrombinase, supporting the idea that NP7 acts by nonspecifically blocking membrane binding sites. Other proteins that inhibit coagulation by this mechanism include annexin V, which binds to PS-containing membranes in a calcium-dependent manner (27,28), and lactadherin which contains the C2 membrane-binding domain found in the coagulation cofactor proteins factor Va and VIIIa (29).

Structure of the Membrane Binding Surface of NP7

The strong salt-concentration dependence of membrane binding, and the lack of any interaction of NP7 with PC vesicles, suggests that binding is mediated by electrostatic interactions of the protein surface with anionic lipid head groups. A positively charged patch corresponding to a helical region of the NP7 model is the apparent site of interaction with the membrane. Unlike the vitamin K-dependent coagulation factors which contain a Gla domain (30), calcium is not required for NP7 binding, and may inhibit binding at higher concentrations. The NP7 model shows no aromatic residues in the vicinity of the basic patch that would suggest a similar mode of binding to that of the C2 domain of factor V, a protein that contains hydrophobic loops surrounded by basic surfaces. It has been proposed that the C2 domain forms nonspecific electrostatic interactions with negative charges in the

membrane that allow aromatic residues in the loops to insert into the membrane and strengthen the binding interaction.

NP7 was found by SPR to rapidly bind a mixed phospholipid monolayer at multiple binding sites having different affinities. This is not surprising because a membrane containing 25% randomly distributed PS would contain multiple spatial arrangements of PS and PC. Polylysine itself has been found to induce domain structures in membranes in which the concentration of PS is enriched relative to its overall concentration in the membrane (31). It is clear from SPR experiments that a subset of high affinity sites is present that allows binding of NP7 at nanomolar concentrations. *R. prolixus* injects a large quantity of salivary protein into its host during feeding. The size of a blood meal has been estimated at approximately 250 μ l and the quantity of salivary protein injected at 60 μ g (J.M.C.R., unpublished observation). The quantity of NP7 in the saliva is not known at this time, but preliminary experiments have shown that several proteins are present that can be sedimented with anionic vesicles at physiologic salt concentrations. These proteins may each have unique individual functions, but may also act together to block coagulation-factor binding sites on activated membranes.

Concluding remarks

R. prolixus saliva is a complex mixture of proteins that contribute overlapping and redundant functions preventing the overall process of blood clotting. Platelet aggregation is inhibited by: apyrase, which hydrolyses ADP; the lipocalin RPAI1, which binds ADP with high affinity (32); a second lipocalin ABP, which binds biogenic amines (33); and NO, which is carried into the circulation by NPs. Coagulation is inhibited by NP2, which binds with factor IXa (34), and NP7, which blocks coagulation factor binding sites on anionic membranes. Preliminary results have shown that other salivary proteins also bind to PS-containing membranes and probably augment the anticoagulant activity of NP7 (J.F.A., unpublished results). The fact that nonspecific blockage of anionic membrane binding sites would affect both the prothrombinase and factor Xase reactions may indicate a more pronounced effect on coagulation than would occur with an inhibitor of a single coagulation reaction. Additionally, the combined effects of the platelet-aggregation inhibitors present in the saliva would act to diminish the procoagulant effect of activated platelets by reducing the degree of platelet activation, and therefore the level of PS exposure on the outer membrane leaflet.

It is remarkable that many of the proteins contained in *R. prolixus* saliva belong to the lipocalin family. A recent study showed more than 25 distinctly different lipocalin genes are expressed in salivary gland tissue, and all contain putative signals for secretion into the lumen of the gland (17). Apparent gene duplication events driven by the need to inhibit the various biochemical processes of hemostasis have led to a large number of structurally divergent lipocalin proteins. Several of these proteins are multifunctional, binding multiple physiologically important ligands and acting on more than one hemostatic process.

Phylogenetic analyses of *R. prolixus* salivary lipocalin sequences have revealed three clades, one of which contains the nitrophorin sequences and the biogenic amine-binding protein (ABP, 17). Within this clade, the sequences have diverged to produce large differences in ligand binding specificity. The nitrophorins bind a heme moiety via iron coordination with His 59 (numbering from NP1), while in ABP His 59 is replaced by asparagine, and the protein binds serotonin, epinephrine and norepinephrine rather than heme (33). In both cases the ligand binding pocket is lined with aromatic amino acid side chains that apparently stabilize the planar, conjugated ring systems of the ligands. Further divergence within the nitrophorin group produced NP2 which binds Factor IX(a) via interaction with its outer

surface (34), and now NP7 which inhibits coagulation by blocking membrane binding sites for coagulation factors.

A second lipocalin clade contains proteins related to the ADP-binding protein RPA11, which is a potent platelet aggregation inhibitor (17,32), while members of the third clade are most similar to triabin, a thrombin inhibitor from the related insect *Triatoma pallidipennis*. Rather than binding a small ligand in the central cavity of the β -barrel, triabin binds with thrombin via its outer surface and inhibits interaction of the substrate prothrombin with the anion-binding exosite of thrombin (35). The function of the triabin-like proteins in *R. prolixus* remains unknown, and no anti-thrombin activity has been detected in the saliva.

Acknowledgments

The authors thank My Van Pham for DNA sequencing, Rosanne Hearn for protein preparation, Bernard Moss for use of the BIAcore instrument, and Nancy Shulman for editorial work on the manuscript.

Abbreviations

PC	phosphatidylcholine
PS	phosphatidylserine
NP	nitrophorin
SNAP	S-nitroso-N-acetylpenicillamine
SPR	surface plasmon resonance

References

1. Nieswandt B, Watson SP. Platelet-collagen interaction: is GPVI the central receptor? *Blood* 2003;102:449–461. [PubMed: 12649139]
2. Brass LF. More pieces of the platelet activation puzzle slide into place. *J Clin Investig* 1999;104:1663–1665. [PubMed: 10606617]
3. Coughlin SR. Protease-activated receptors in vascular biology. *Thromb Haemost* 2001;86:298–307. [PubMed: 11487018]
4. Sims PJ, Wiedmer T. Unraveling the mysteries of phospholipid scrambling. *Thromb Haemost* 2001;86:266–275. [PubMed: 11487015]
5. Zwaal RF, Comfurius P, Bevers EM. Mechanism and function of changes in membrane-phospholipid asymmetry in platelets and erythrocytes. *Biochem Soc Trans* 1993;21:248–253. [PubMed: 8359475]
6. Martin S, Pombo I, Poncet P, David B, Arock M, Blank U. Immunologic stimulation of mast cells leads to the reversible exposure of phosphatidylserine in the absence of apoptosis. *Int Arch Allergy Immunol* 2000;123:249–258.
7. Demo SD, Masuda E, Rossi AB, Thronset BT, Gerard AL, Chan EH, Armstrong RJ, Fox BP, Lorens JB, Payan DG, Scheller RH, Fisher JM. Quantitative measurement of mast cell degranulation using a novel flow cytometric annexin-V binding assay. *Cytometry* 1999;36:340–348. [PubMed: 10404150]
8. Ribeiro JMC, Hazzard JMH, Nussenzveig RH, Champagne DE, Walker FA. Reversible binding of nitric oxide by a salivary heme protein from a bloodsucking insect. *Science* 1993;260:539–541. [PubMed: 8386393]
9. Andersen JF, Ding XD, Balfour C, Shokhireva TK, Champagne DE, Walker FA, Montfort WR. Kinetics and equilibria in ligand binding by nitrophorins 1–4: evidence for stabilization of a nitric oxide-ferriheme complex through a ligand-induced conformational trap. *Biochemistry* 2000;39:10118–10131. [PubMed: 10956000]

10. Flower DR. The lipocalin protein family: Structure and function. *Biochem J* 1996;318:1–14. [PubMed: 8761444]
11. Flower DR, North AC, Sansom CE. The lipocalin protein family: Structural and sequence overview. *Biochem Biophys Acta* 2000;1482:9–24. [PubMed: 11058743]
12. Weichsel A, Andersen JF, Champagne DE, Walker FA, Montfort WR. Crystal structures of a nitric oxide transport protein from a blood-sucking insect. *Nature Struct Biol* 1998;5:304–309. [PubMed: 9546222]
13. Ding XD, Weichsel A, Andersen JF, Shokhireva TK, Balfour C, Pierik AJ, Averill BA, Montfort WR, Walker FA. Nitric oxide binding to the ferri- and ferroheme states of nitrophorin 1, a reversible NO-binding heme protein from the saliva of the blood-sucking insect *Rhodnius prolixus*. *J Am Chem Soc* 1999;121:128–138.
14. Zhang Y, Ribeiro JM, Guimaraes JA, Walsh PN. Nitrophorin-2: a novel mixed-type reversible specific inhibitor of the intrinsic factor-X activating complex. *Biochemistry* 1998;37:10681–10690. [PubMed: 9692958]
15. Isawa H, Yuda M, Yoneda K, Chinzei Y. The insect salivary protein, prolixin-S, inhibits factor IXa generation and Xase complex formation in the blood coagulation pathway. *J Biol Chem* 2000;275:6636–6641. [PubMed: 10692472]
16. Ribeiro JMC, Walker FA. High affinity histamine-binding and antihistaminic activity of the salivary nitric oxide-carrying heme protein (nitrophorin) of *Rhodnius prolixus*. *J Exp Med* 1994;180:2251–2257. [PubMed: 7964498]
17. Ribeiro JMC, Andersen J, Silva-Neto MAC, Pham VM, Garfield MK, Valenzuela JG. Exploring the sialome of the blood-sucking bug *Rhodnius prolixus*. *Ins Biochem Mol Biol* 2004;34:61–79.
18. Nielsen H, Engelbrecht J, Brunak S, Heijne G. Identification of prokaryotic and eukaryotic signal peptides and prediction of their cleavage sites. *Protein Eng* 1997;10:1–6. [PubMed: 9051728]
19. Andersen JF, Champagne DE, Weichsel A, Ribeiro JMC, Balfour CA, Dress V, Montfort WR. Nitric oxide binding and crystallization of recombinant nitrophorin 1, a nitric oxide transport protein from the blood-sucking bug. *Rhodnius prolixus*, *Biochemistry* 1997;36:4423–4428.
20. Disalvo EA, Campos AM, Abuin E, Lissi EA. Surface changes induced by osmotic shrinkage on large unilamellar vesicles. *Chem Phys Lipids* 1996;84:35–45. [PubMed: 8952051]
21. Francischetti IM, Andersen JF, Ribeiro JM. Biochemical and functional characterization of recombinant *Rhodnius prolixus* platelet aggregation inhibitor 1 as a novel lipocalin with high affinity for adenosine diphosphate and other adenine nucleotides. *Biochemistry* 2002;41:3810–3818. [PubMed: 11888300]
22. Andersen JF, Montfort WR. The crystal structure of nitrophorin 2: A trifunctional antihemostatic protein from the saliva of *Rhodnius prolixus*. *J Biol Chem* 2000;275:30496–30503. [PubMed: 10884386]
23. Honig B, Nicholls A. Classical electrostatics in biology and chemistry. *Science* 1995;268:1144–1149. [PubMed: 7761829]
24. Nicholls A, Bharadwaj R, Honig B. GRASP - Graphical representation and analysis of surface properties. *Biophys J* 1993;64:A166.
25. Callahan MK, Williamson P, Schlegel RA. Surface expression of phosphatidylserine on macrophages is required for phagocytosis of apoptotic thymocytes. *Cell Death Differ* 2000;7:645–653.
26. Hirt UA, Leist M. Rapid, noninflammatory, and PS-dependent phagocytic clearance of necrotic cells. *Cell Death Differ* 2003;10:1156–1164.
27. Mo Y, Campos B, Mealy TR, Commodore L, Head JF, Dedman JR, Seaton BA. Interfacial basic cluster in annexin V couples phospholipid binding and trimer formation on membrane surfaces. *J Biol Chem* 2003;278:2437–2443. [PubMed: 12401794]
28. London F, Ahmad SS, Walsh PN. Annexin V inhibition of factor IXa-catalyzed factor X activation on human platelets and on negatively-charged phospholipid vesicles. *Biochemistry* 1996;35:16886–16897. [PubMed: 8988028]
29. Shi J, Gilbert GE. Lactadherin inhibits enzyme complexes of blood coagulation by competing for phospholipid-binding sites. *Blood* 2003;101:2628–2636. [PubMed: 12517809]

30. Zwaal RF, Comfurius P, Bevers EM. Lipid-protein interactions in blood coagulation. *Biochem Biophys Acta* 1998;1376:433–453. [PubMed: 9805008]
31. Denisov G, Wanaski S, Luan P, Glaser M, McLaughlin S. Binding of basic peptides to membranes produces lateral domains enriched in the acidic lipids phosphatidylserine and phosphatidylinositol 4,5-bisphosphate: an electrostatic model and experimental results. *Biophys J* 1998;74:731–744. [PubMed: 9533686]
32. Francischetti IM, Ribeiro JM, Champagne D, Andersen J. Purification, cloning, expression, and mechanism of action of a novel platelet aggregation inhibitor from the salivary gland of the blood-sucking bug, *Rhodnius prolixus*. *J Biol Chem* 2000;275:12639–12650. [PubMed: 10777556]
33. Andersen JF, Francischetti IMB, Valenzuela JG, Schuck P, Ribeiro JMC. Inhibition of hemostasis by a high affinity biogenic amine-binding protein from the saliva of a blood-feeding insect. *J Biol Chem* 2003;278:4611–4617. [PubMed: 12464610]
34. Ribeiro JMC, Schneider M, Guimaraes JA. Purification and characterization of prolixin S (nitrophorin 2), the salivary anticoagulant of the bloodsucking bug *Rhodnius prolixus*. *Biochem J* 1995;308:243–249. [PubMed: 7755571]
35. Fuentes-Prior P, Noeske-Jungblut C, Donner P, Schleuning WD, Huber R, Bode W. Structure of the thrombin complex with triabin, a lipocalin-like exosite-binding inhibitor derived from a triatomine bug. *Proc Natl Acad Sci USA* 1997;94:11845–11850. [PubMed: 9342325]

```

1                               60
NP2 MELYTALLAVTILCLTSTMGVSGDCSTNISPKQGLDKAKYFSGK.WYVTHFLDKDPQ.VT
NP3 MEPYSALLAVTILCLTSTMGVSGDCSTNISPKKGLDKAKYFSGT.WYVTHYLDKDPQ.VT
NP4 MKSYTSL LAVAILCLFG..GVNGACTKNAIAQTGFNKDKYFNGDVWYVTDYLDLEPDDVP
NP7 MELYTALLAVTILSPSSIVGLPGECSVNVIPKKNLDKAKFFSGT.WYETHYLDMDPQ.AT

61                               120
NP2 DQYCSSFTPRES DGTVKEALYHYNANKKTSFYNI GEGKLESSGLQYTAKYKTVDKKKAVL
NP3 DPYCSSFTPKESGGTVKEALYHFNSKKKTSFYNI GEGKLGSSGVQYTAKYNTVDKKRKEI
NP4 KRYCAALAAGTASGKLKEALYHYDPKTQDTFYDVSELQVESLG.KYTANFKKVDKNGNVK
NP7 EKFCFSFAPRESGGTVKEALYHFNVDSKVSFYNTGTGPLESNGAKYTAKFNTVDKKGKEI

121                               180
NP2 KEADEKNSYTLTVLEADDSSALVHICLREGSKDLGDLYTVLTHQKDAEPS AKVKSAVTQA
NP3 EPADPKDSYTLTVLEADDSSALVHICLREGPKDLGDLYTVLSHQKTGEPS ATVKNAVAQA
NP4 VAVTAGNYTFTVMYADDSSALIHTCLHKGKNDLGDLYAVLNRNKDAAAG DKVKSAVSAA
NP7 KPADEKYSYTVTVIEAAKQSALIHICLQEDGKDIDGLYSVLNRNKNALPN KIKKALNKV

181
NP2 GLQLSQFVGTKDLGCGYDDQFTSL
NP3 GLKLNDFVDTKTLSCYDDQFTSM
NP4 TLEFSKFISTKENNCAYDNDLSKSLTK
NP7 SLVLTKFVVTKDLDCYDDKFLSSWQK

```

Figure 1.

Alignment of the NP7 amino acid sequence with NP2–4. The predicted signal peptide for NP7 is underlined. The sequence corresponding to the putative membrane-binding helix is boxed in blue in the NP7 sequence. The position of the K149A mutant is shown in green. The comparable sequences in NP2–4 are boxed in red.

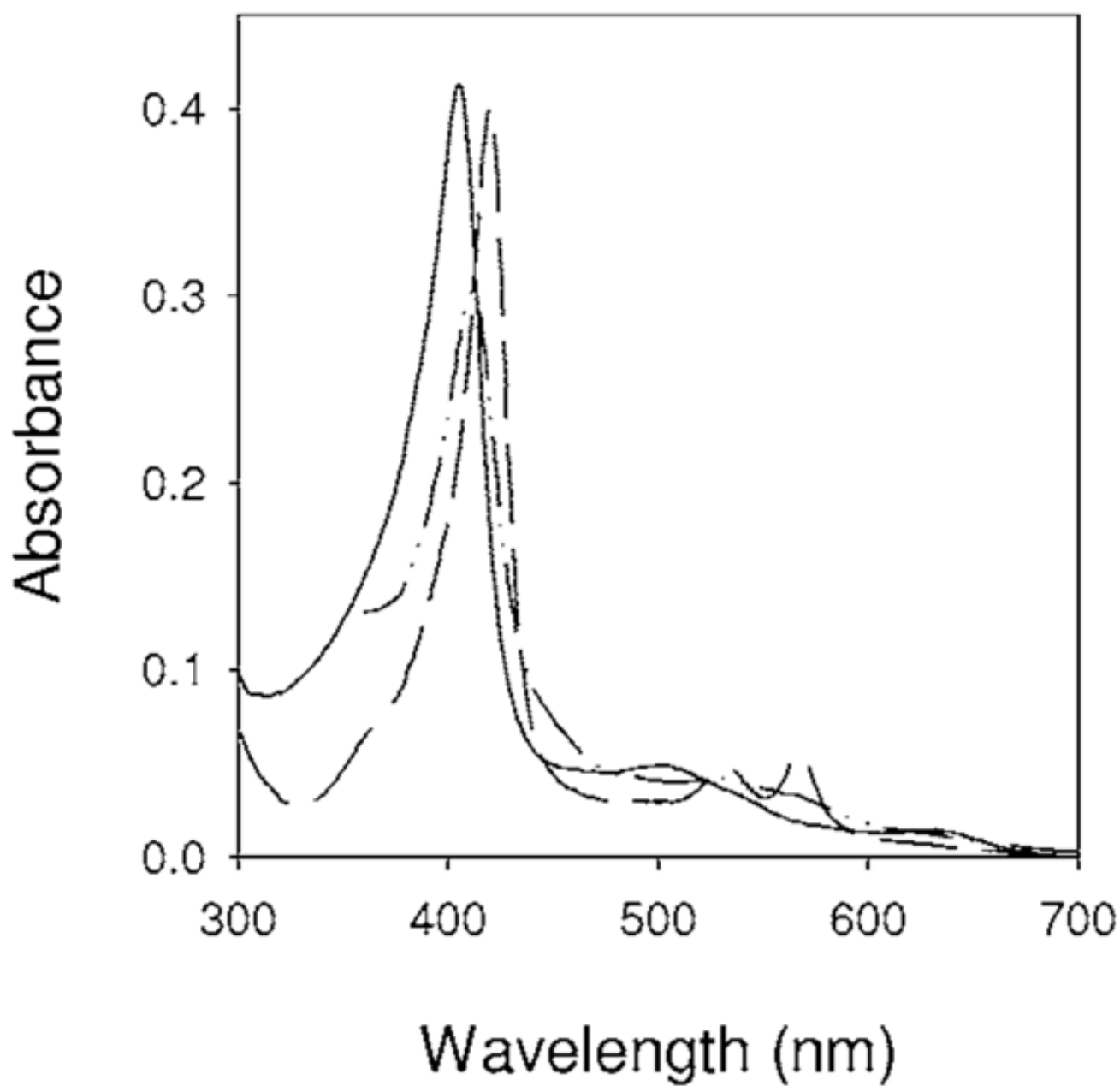


Figure 2.

NO and histamine complex formation with NP7 showing shift of the Soret maximum from 403 nm to 420 nm in the case of NO (-----) and 412 nm in the case of histamine (..-.-.-.).

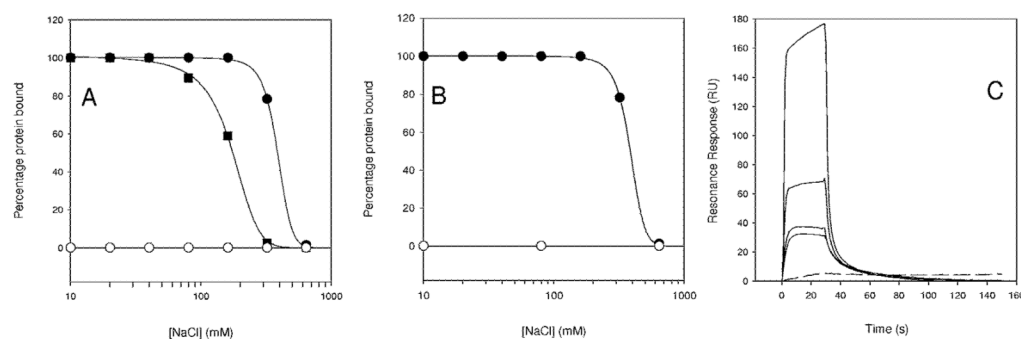
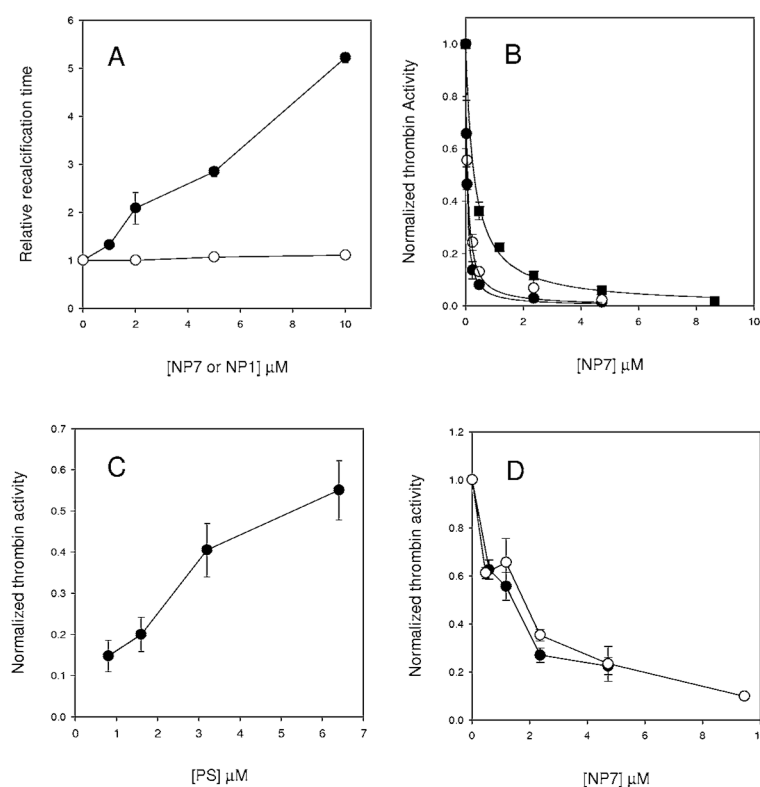


Figure 3.

Binding of NPs with phospholipid vesicles as measured by sedimentation and SDS-PAGE. All assays were performed in 20 mM Tris-HCl, pH 7.5 containing the indicated concentrations of NaCl. In all cases, the phospholipid concentration was 0.5 mg/ml and the protein concentration was 3 μ M. (A) Relationship of NP7 binding with buffer concentration of NaCl at various compositions of phospholipid. Filled circles: 100 % PS vesicles; filled squares: 3:1 PC:PS vesicles; open circles: 100 % PC vesicles. (B) Relationship of binding with NaCl concentration for NP1, NP2, NP3 and NP7, using 100 % PS vesicles. Filled circles: NP7; open circles: NP1, 2, 3. (C) Interaction of NP7 with a 3:1 PC:PS monolayer using surface plasmon resonance. Sensorgrams obtained with 30, 60, 200, and 600 nM NP7 are shown as solid lines. Sensorgram obtained with 220 nM NP3 is shown as a dashed line.

**Figure 4.**

Anticoagulant activity of NP7. Each point represents the mean of three determinations. (A) Recalcification time of platelet-rich plasma (PRP) in the presence of NP7 and NP1. Citrated PRP was incubated with NP7 or NP1 as described in Materials and Methods, followed by addition of CaCl_2 to a concentration of 5 mM. Filled circles, NP7; open circles, NP1. (B) Inhibition of reconstituted prothrombinase using various concentrations of 100% PS vesicles as a source of phospholipid. Thrombin generation was measured by the rate of hydrolysis of the chromogenic substrate S-2238. The relative thrombin activity is the rate of hydrolysis by thrombin formed in the presence of the indicated concentrations of NP7, divided by the rate formed in the absence of NP7. Filled circles, 0.5 μM PS; open circles, 1.0 μM PS; filled squares, 15 μM PS. (C) Relationship of prothrombinase inhibition with phospholipid concentration at a NP7 concentration of 230 nM, using 100% PS vesicles as a source of phospholipid. (D) Inhibition of prothrombinase activity using 3:1 PC:PS vesicles (1 μM) or collagen-activated platelets (1.5×10^6 platelets in a final volume of 130 μl). Open circles: Prothrombinase activity (measured as rate of S-2238 hydrolysis) as a function of NP7 concentration in the presence of 3:1 PC:PS vesicles. Closed circles: Prothrombinase activity as a function of NP7 concentration with activated platelets serving as a source of phospholipid.

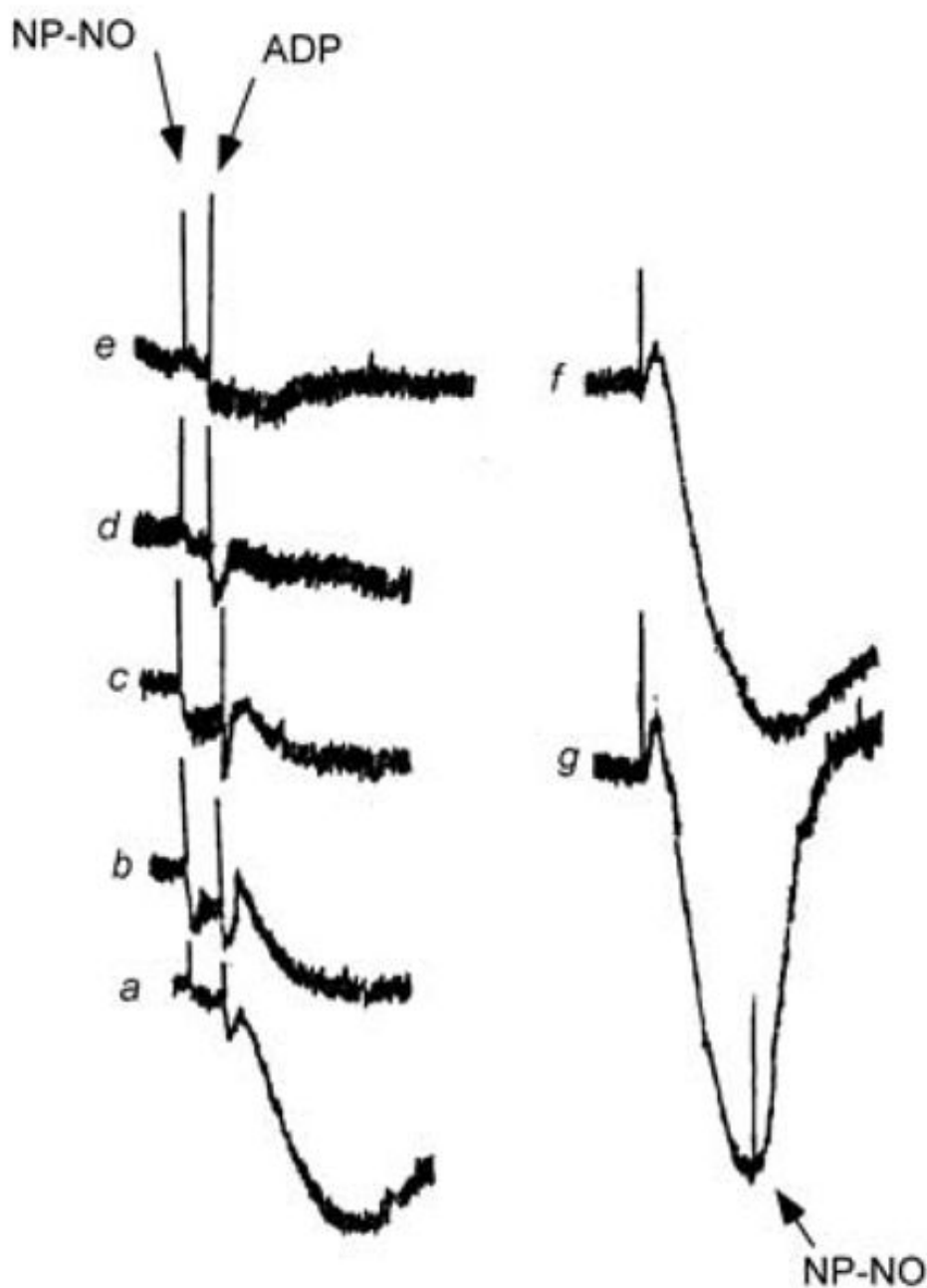
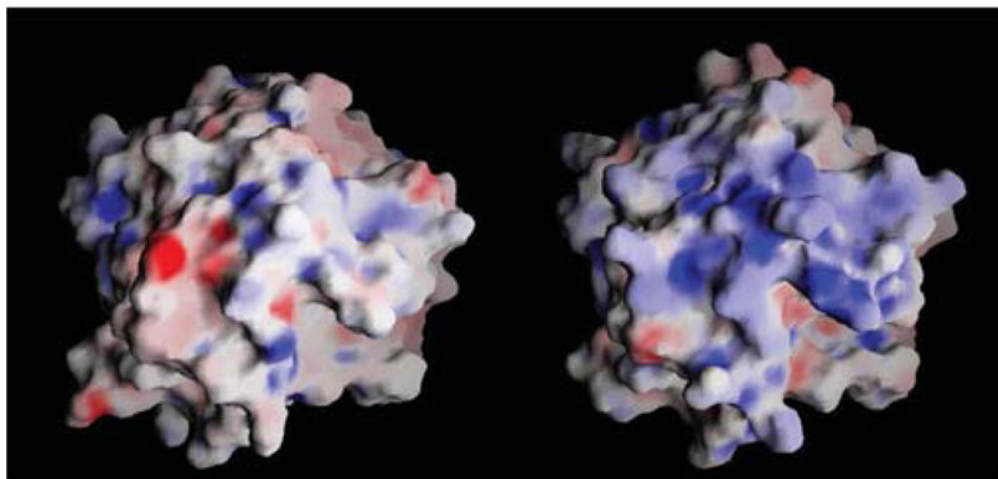
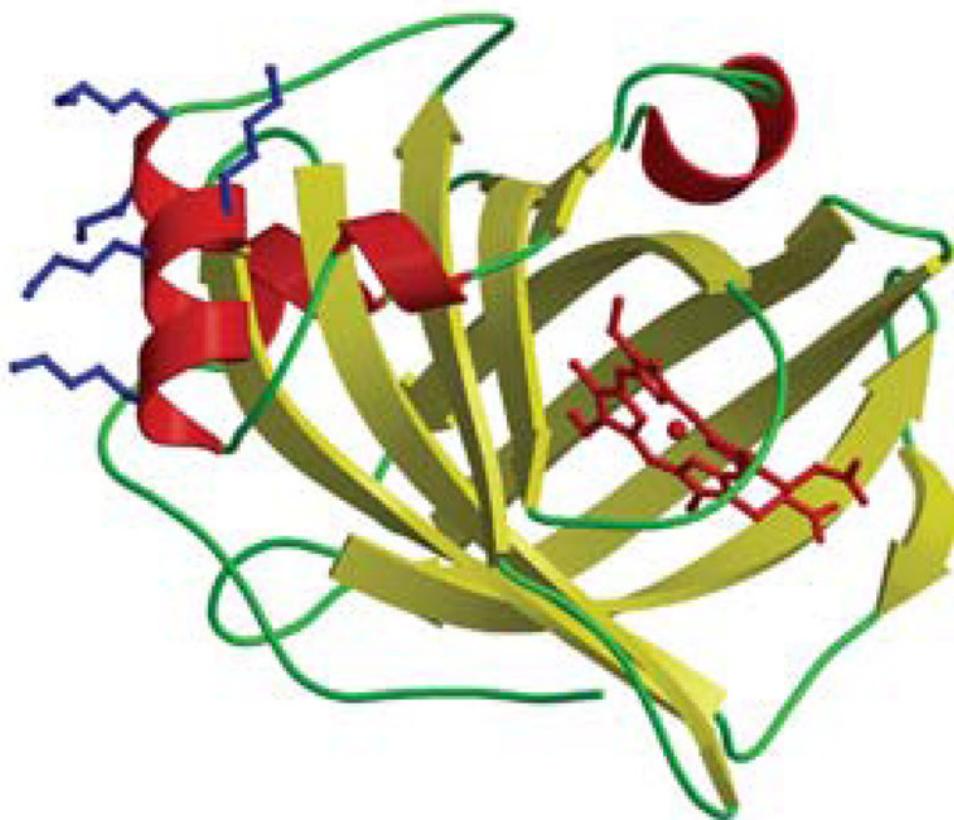


Figure 5.

Inhibition of ADP-induced platelet aggregation by the NP7-NO complex as measured in an aggregometer. Washed platelets were treated with either NP7-NO complex or buffer (20 mM sodium acetate, pH 4.5 150 mM NaCl), then stimulated with ADP (3 μ M). Concentrations of NP7-NO complex: a), 0 nM; b), 1 nM; c), 10 nM; d), 40 nM; e), 400 nM. Platelets were stimulated with ADP (3 μ M), allowed to aggregate, then left untreated (f) or treated with NP7-NO complex (400 nM, g).

Fig 6A**Fig 6b****Figure 6.**

Molecular modeling of NP7. Models were constructed using the coordinates of the NP2 crystal structure (PDB accession number 1EUO (22)) with Swiss-Model. Heme was manually placed in model by superposition with NP2. Electrostatic potentials were calculated using DelPhi and a surface map was generated using GRASP.

(A) Electrostatic potential surfaces of NP2 (left) and NP7 (right) showing the positively charged surface (blue) corresponding to the putative membrane interaction region.

(B) Ribbon diagram of the NP7 model with lysine side chains (blue) highlighted on the external helix corresponding to the basic surface shown in Figure 6a.

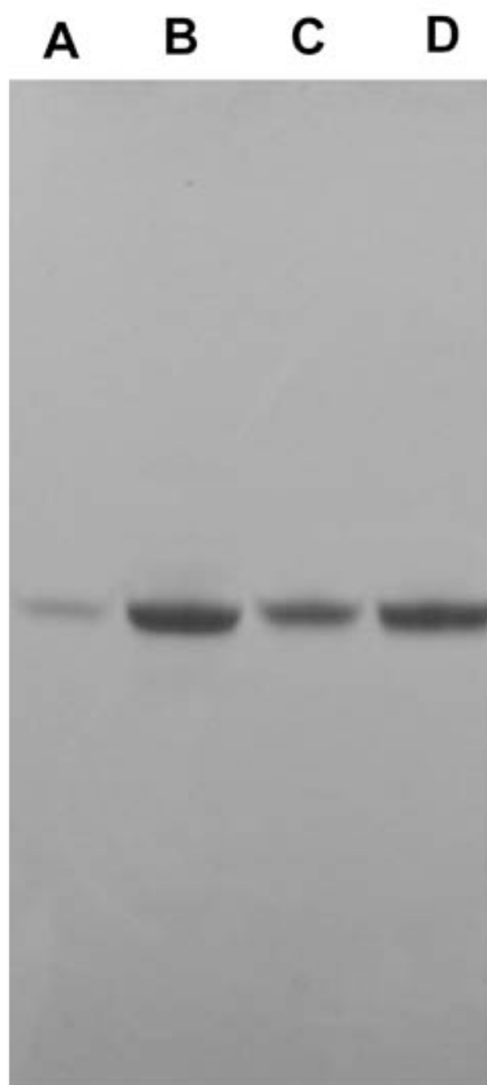


Figure 7. Sedimentation by ultracentrifugation of NP7 (K149A mutant) and NP7 (wild type) bound to 3:1 PC:PS vesicles at 200 mM NaCl. After sedimentation the supernatant was removed, and the pellet suspended in buffer and both were analyzed by SDS-PAGE with Coomassie blue staining. Lane A: NP7(K149A) pellet, Lane B: NP7 (K149A) supernatant, Lane C: NP7 (wild type) pellet, Lane D: NP7 (wild type) supernatant.

Table 1

Two-binding site kinetic (\pm S.E.) and binding parameters for interaction of NP7 with a PC:PS (3:1) monolayer determined by surface plasmon resonance.

	k_{on}^a	k_{off}^b	K_d^c
1	$4.9 (1.3) \times 10^5$	0.37 (0.02)	755
2	$8.3 (0.9) \times 10^6$	0.04 (0.001)	4.8

$^a M^{-1} s^{-1}$

$^b s^{-1}$

$^c nM$